Helix Induction and Springboard Strain in Peptide-Sandwiched Mesohemes[1]

Paige A. Arnold,[†,2] David R. Benson,*[,†] Daniel J. Brink,[†] Michael P. Hendrich,[‡] Gouri S. Jas,[†] Michelle L. Kennedy,[†] Doros T. Petasis,[‡] and Manxue Wang[†,2]

Departments of Chemistry, University of Kansas, Lawrence, Kansas 66045, and Carnegie Mellon University, Pittsburgh, Pennsylvania 15213

Received April 25, 1996[⊗]

We report the results of studies of a series of water-soluble peptide adducts of iron mesoporphyrin IX (FeMPIX). In one group of compounds, the peptide-sandwiched mesohemes (PSMs; **1**−**5**), two identical 13-residue peptides are connected to the propionate groups of FeMPIX via amide linkages with Nϵ nitrogens of lysine (Lys) residues. The corresponding monopeptide analogues of each PSM (**1m**−**5m**) have also been prepared. The imidazolyl side chain of a histidine (His) residue in each peptide coordinates to the mesohemin iron. The compounds differ from one another in the relative positions of the His and Lys residues in the peptide sequences. In **1**, **2**, **4**, and **5** and the corresponding monopeptide systems, Fe−His coordination results in various extents of peptide helix induction in neutral aqueous solution. The peptides in **3** and **3m** remain in random coil conformations. Helix content in **1**−**5** can be enhanced by addition of organic cosolvents, including 2,2,2-trifluoroethanol (TFE) and 1-propanol (PrOH). Data from EPR spectroscopy and from pH titrations suggest that in aqueous solution the folded forms of **3** and **5** (in which both Fe−His bonds are intact) are less stable than the folded forms of the other PSMs. Addition of TFE or PrOH increases the stability of the folded forms of **1**, **2**, and **4** by favoring helical conformations for the peptides whether or not the Fe−His bonds are intact, thus eliminating the helix unwinding that occurs upon bond breakage in aqueous solution. Increasing peptide helix content in **3** and **5** with TFE does little or nothing to increase the stability of their folded forms, consistent with the prediction that the His−Lys spacing in these compounds is not compatible with stable helical conformations for the peptides. UV/vis spectra of the Fe(II) complexes of **3** and **5** are also consistent with reduced structural stability of these PSMs, as a sizable population of pentacoordinate (high-spin) Fe(II) is in equilibrium with hexacoordinate (low-spin) Fe(II) at neutral pH, both in aqueous solution and in the presence of 30% (v/v) TFE at 8 °C. The Fe(II) complexes of **1**, **2**, and **4** remain predominantly hexacoordinate in both solvent systems.

Introduction

Juxtaposition of heme groups with α-helices bearing histidine (His) ligands is a common motif both in natural[3] and in *de novo* designed[4] hemoproteins. Other amino acids interact with the heme via hydrophobic, ionic, or covalent interactions, the sum of these interactions serving to define the chemical and physical properties of the heme. The combined interactions also confer stabilization on the hemoprotein tertiary structure.[5]

In hemoproteins, the heme binding site is defined by the three-dimensional fold of the apoprotein.[6] Thus, the heme iron must coordinate to protein-based ligands in the geometry that is enforced by this fold, often leading to strained metal−ligand bonds (the "entatic" state defined by Vallee and Williams).[7] In hemoglobins, strain in the bond between heme iron and the proximal His regulates binding of dioxygen.[8] Strain may also play a role in NO-mediated activation of guanylate cyclase (GC), which occurs via displacement of His coordinated to heme iron,[9] with a subsequent protein conformational change.[10] Fe−His bond strain has been studied in several model hemoprotein systems.[11] Traylor and co-workers investigated the effect of strain on Fe−His bonds in models of T-state hemoglobin.[12] In

† University of Kansas.
‡ Carnegie Mellon University.
⊗ Abstract published in *Advance ACS Abstracts,* October 15, 1997.

(1) First paper in this series: Benson, D. R.; Hart, B. R.; Zhu, X.; Doughty, M. B. *J. Am. Chem. Soc.* **1995**, *117*, 8502−8510.
(2) These two individuals contributed equally to this work.
(3) For example, see the following. (a) Myoglobin: Takano, T. *J. Mol. Biol.* **1977**, *110*, 569−584. (b) Hemoglobin: Ladner, R. C.; Heidner, E. J.; Perutz, M. F. *J. Mol. Biol.* **1977**, *114*, 385−414. (c) Cytochrome b562: Lederer, F.; Glatigny, A.; Bethge, P. H.; Bellamy, H. D.; Mathews, F. S. *J. Mol. Biol.* **1981**, *148*, 427−448. (d) Cytochrome *c′*: Finzel, B. C.; Weber, P. C.; Hardman, K. D.; Salemme, F. R. *J. Mol. Biol*. **1985**, *186*, 627−643. (e) Cytochrome *c*3: Higuchi, Y.; Kusunoki, M.; Matsuura, Y.; Yasuoka, N.; Kakudo, M. *J. Mol. Biol.* **1984**, *172*, 109−139. (f) Cytochrome *c* peroxidase: Goodin, D. B.; McRee, D. E. *Biochemistry* **1993**, *32*, 3313−3324. (g) Myeloperoxidase: Zeng, J.; Fenna, R. E. *J. Mol. Biol.* **1992**, *226*, 185−207. (h) Cytochrome *c* oxidase: Tsukihara, T.; Aoyama, H.; Yamashita, E.; Tomizaki, T.; Yamaguchi, H.; Shinzawa-Itoh, K.; Nakashima, R.; Yaono, R.; Yoshikawa, S. *Science* **1995**, *269*, 1069−1074. Iwata, S.; Ostermeier, C.; Ludwig, B.; Michel, H. *Nature* **1995**, *376*, 660−669.
(4) (a) Arnold, P. A.; Shelton, W. R.; Benson, D. R. *J. Am. Chem. Soc.* **1997**, *119*, 3181−3182. (b) Nastri, F.; Lombardi, A.; Morelli, G.; Maglio, O; D'Auria, G.; Pedone, C.; Pavone, V. *Chem. Eur. J.* **1997**, *3*, 340−349. (c) D'Auria, G.; Maglio, O.; Nastri, F.; Lombardi, A.; Mazzeo, M.; Morelli, G.; Paolillo, L.; Pedone, C.; Pavone, V. *Chem. Eur. J.* **1997**, *3*, 350−362. (d) Sakamoto, S.; Sakurai, S.; Ueno, A.; Mihara, H. *Chem. Commun.* **1997**, 1221−1222. (e) Gibney, B. R.; Mulholland, S. E.; Rabanal, F.; Dutton, P. L. *Proc. Natl. Acad. Sci. U.S.A.* **1996**, *93*, 15041−15046. (f) Rabanal, F.; DeGrado, W. F.; Dutton, P. L. *J. Am. Chem. Soc.* **1996**, *118*, 473−474. (g) Robertson, D. E.; Farid, R. S.; Moser, C. C.; Urbauer, J. L.; Mulholland, S. E.; Pidikiti, R.; Lear, J. D.; Wand, A. J.; DeGrado, W. F.; Dutton, P. L. *Nature (London)* **1994**, *368*, 425−432. (h) Choma, C. T.; Lear, J. D.; Nelson, M. J.; Dutton, P. L.; Robertson, D. E.; DeGrado, W. F. *J. Am. Chem. Soc.* **1994**, *116*, 856−865.
(5) (a) Hargrove, M. S.; Olson, J. S. *Biochemistry* **1996**, *35*, 11310−11318. (b) Storch, E. M.; Daggett, V. *Biochemistry* **1996**, *35*, 11596−11604 and references therein.
(6) Lumry, R.; Eyring, H. *J. Phys. Chem.* **1954**, *58*, 110−120. See also: Huber, R. *Eur. J. Biochem.* **1990**, *187*, 283−305.
(7) Vallee, B. L.; Williams, R. J. P. *Proc. Natl. Acad. Sci. U.S.A.* **1968**, *59*, 498−505.
(8) (a) Perutz, M. F.; Fermi, G.; Luisi, B.; Shaanan, B.; Liddington, R. C. *Acc. Chem. Res.* **1987**, *20*, 309−321. (b) Royer, W. E., Jr. *J. Mol. Biol.* **1994**, *235*, 657−681.
(9) Deinum, G.; Stone, J. R.; Babcock, G. T.; Marletta, M. A. *Biochemistry* **1996**, *35*, 1540−1547.
(10) Traylor, T. G.; Sharma, V. S. *Biochemistry* **1992**, *31*, 2847−2849.

S0020-1669(96)00444-2 CCC: $14.00

Chart 1

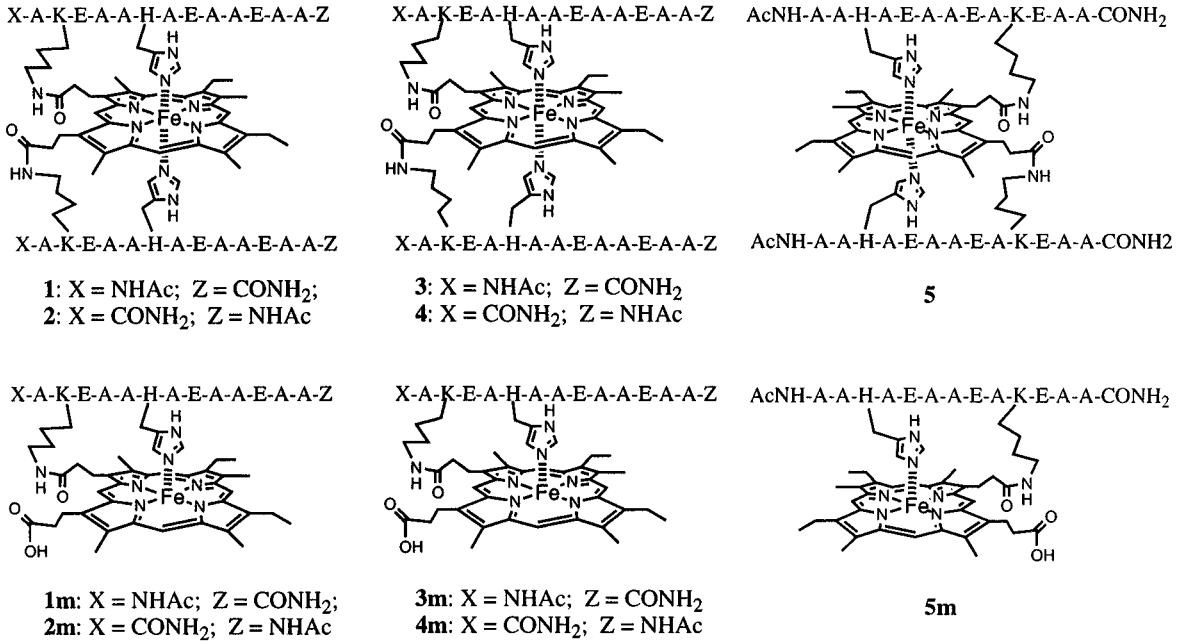

these systems, strain is manifested as stretching and/or bending of the Fe−His bonds brought about by ring strain, face strain, and/or springboard strain.[12] Springboard strain occurs when energetically unfavorable conformations are required of the linkers connecting the ligands to the heme propionate groups. This results in a tendency of the chelate ring to "spring open."[12a]

Systematic examination of the influence of heme−protein interactions on hemoprotein structure and function is complicated by their large size and structural complexity. As an approach to unraveling these effects, we have developed a class of synthetic hemoprotein models dubbed peptide-sandwiched mesohemes (PSMs; **1**−**5** in Chart 1).[1] Each PSM consists of two identical peptides covalently linked to the propionate groups of iron(III) mesoporphyrin IX via amide linkages with lysine (Lys) Nϵ amines. A His residue in each peptide coordinates to the heme iron. When both His ligands are coordinated to Fe, a PSM is considered to be "folded". Rupture of one or both Fe−His bonds leads to an "unfolded" form. In the folded forms of **1**, **2**, **4**, and **5**, both peptides adopt conformations having varying degrees of α-helix content. Helix content can be increased through the use of organic cosolvents such as 2,2,2-trifluoroethanol (TFE) or 1-propanol (PrOH), leading to substantial stabilization of the folded forms of **1**, **2**, and **4**. The cosolvents aid in stabilization by favoring helical conformations in the peptides in both the presence and the absence of Fe−His coordination. Stabilization in these PSMs is thus attributed to a reduction in the tendency of the helical peptides to unwind upon rupture of the Fe−His bonds, an interesting variation on Traylor's concept of springboard strain.[12a]

Using a variety of spectroscopic techniques, we have found that the folded forms of **3** and **5** are less stable than the folded forms of **1**, **2**, and **4**, even when helicity in the peptides is increased by the addition of TFE or PrOH. This also is attributed to a manifestation of Traylor's springboard strain, resulting from the fact that, in **3** and **5**, spacing between His and Lys does not allow for formation of stable peptide helices.

This work represents a synthesis of concepts developed more than 30 years apart: the attachment of ligand-bearing groups to porphyrins for use as model hemoproteins[11] and the use of conformational constraints to induce α-helicity in short monomeric peptides.[13−15] Previously reported methods for providing conformational constraints include coordination of metal ions between amino acid side chains,[13] formation of intrapeptide covalent linkages,[14] and use of rigid organic templates.[15]

Experimental Section

General Considerations. All reagents were of commercial grade and were used without further purification except for dimethyl sulfoxide (DMSO), which was dried over 4 Å molecular sieves. Rink resin was purchased from Advanced Chemtech (Louisville, KY). Amino acids were from either Advanced Chemtech (Louisville, KY) or Bachem (San Diego, CA).

Peptide Synthesis. Peptides for PSMs **1**−**5** were prepared on a Rainin PS3 automated synthesizer using Fmoc chemistry[16] on Rink resin (100−200 mesh, 1% DVB, substitution level 0.56−0.62 mmol/g). All peptides were deprotected and cleaved from resin using Reagent K.[17] Purification was accomplished by HPLC (Rainin system HPLX) on a 2.2 cm Vydac C18 peptide/protein column using a gradient of acetonitrile in 0.1% aqueous TFA (5% to 40% over 40 min) at a flow rate of 8 mL/min. Amino acid analyses for peptide components of PSMs are as follows [AA, found (calc)]. **1**: A, 7.81 (8); E, 3.15 (3);

(11) (a) Reviewed in: Morgan, B.; Dolphin, D. *Struct. Bonding (Berlin)* **1987**, *64*, 115−203. (b) See also: Casella, L.; Fantucci, P.; Gullotti, M.; De Gioia, L.; Strini, A.; Chillemi, F. *Inorg. Chem.* **1996**, *35*, 439−444.

(12) (a) Geibel, J.; Cannon, J.; Campbell, D.; Traylor, T. G. *J. Am. Chem. Soc.* **1978**, *100*, 3575−3585. (b) Traylor, T. G. *Acc. Chem. Res.* **1981**, *14*, 102−109.

(13) (a) Ghadiri, M. R.; Fernholz, A. K. *J. Am. Chem. Soc.* **1990**, *112*, 9633−9635. (b) Ghadiri, M. R.; Choi, C. *J. Am. Chem. Soc.* **1990**, *112*, 1630−1632. (c) Ruan, F.; Chen, Y.; Hopkins, P. B. *J. Am. Chem. Soc.* **1990**, *112*, 9403−9404.

(14) (a) Phelan, J. C.; Skelton, N. J.; Braisted, A. C.; McDowell, R. S. *J. Am. Chem. Soc.* **1997**, *119*, 455−460. (b) Jackson, D. Y.; King, D. S.; Chmielewski, J.; Singh, S.; Schultz, P. G. *J. Am. Chem. Soc.* **1991**, *113*, 9391−9392. (c) Osapay, G.; Taylor, J. W. *J. Am. Chem. Soc.* **1992**, *114*, 6966−6973. (d) Chorev, M.; Roubini, E.; McKee, R. L.; Gibbons, S. W.; Goldman, M. E.; Caulfield, M. P.; Rosenblatt, M. *Biochemistry* **1991**, *30*, 5968−5974.

(15) Kemp, D. S.; Allen, T. J.; Oslick, S. L. *J. Am. Chem. Soc.* **1995**, *117*, 6641−6657.

(16) Fields, G. B.; Noble, R. L. *Int. J. Peptide Protein Res.* **1990**, *35*, 161−214.

(17) King, D. S.; Fields, C. G.; Fields, G. B. *Int. J. Peptide Protein Res.* **1990**, *36*, 255−266.

H, 1.03 (1); K, 1.01(1). **2**: A, 8.00 (8); H, 1.10 (1); E, 3.02 (3); K, 0.99 (1). **3**: A, 8.00 (8); H, 1.01 (1); E, 3.00 (3); K, 0.92 (1). **4**: A, 8.23 (8); H, 1.10 (1); E, 3.00 (3); K, 0.92 (1). **5**: A, 7.72 (8); H, 1.25 (1); E, 3.43 (3); K, 1.00 (1). All peptides were homogeneous as determined by analytical HPLC and by fast atom bombardment mass spectrometry (FAB-MS). FAB-MS measurements were made on a VG AutoSpec with a high-resolution double sector. Amino acid analyses were performed by the KU Biochemical Research Services Laboratory using FITC precolumn derivatization of peptides hydrolyzed in 6 M HCl (0.01% phenol) for 24 h.

General Method for Synthesis of PSMs 1−5 and Monopeptide Adducts 1m−5m. The dry peptide (6 mg, 4.8 μmol) was dissolved in 80 μL of dry DMSO in a microcentrifuge tube. Diisopropylethylamine (18 μL, 105 μmol) was added followed by iron(III) mesoporphyrin IX bis(*p*-nitrophenyl) ester[1] (1 mg, 1.2 μmol). The mixture was vortexed for several seconds to give a red-brown solution and then warmed at 40 °C for 3 h. The solution was diluted with 500 μL of 50 mM ammonium acetate and purified by sequential ion exchange chromatography (Sephadex CM50; 50 mM ammonium acetate), reverse-phase HPLC (Vydac 1.0 cm C4 peptide/protein column using a gradient of acetonitrile in 10 mM aqueous ammonium acetate, 10% to 40% over 40 min at 2.0 mL/min), and size exclusion chromatography (Sephadex G25, fine). FAB-MS of **1**−**5**: *m*/*z* 3145 (MH^+). The monopeptide analogues of PSMs **1** (**1m**), **2** (**2m**), and **5** (**5m**) were isolated during purification of the respective PSMs. Monopeptide adducts **3m** and **4m** were prepared using the general method described above for the PSMs, except that only 1.2 equiv of peptide was used. FAB-MS of **1m**−**5m**: *m*/*z* 1882 (MH^+).

Molecular Modeling Studies. The Sybyl suite of molecular modeling programs was employed,[18] with the Kollman all-atom force field used in energy minimizations. Modeling of the heme portion of the PSMs was performed using iron protoporphyrin IX from the X-ray structure of *Aplysia limacina* metmyoglobin,[19] with the proximal His (95) ligand attached and with the vinyl groups of the porphyrin converted to methyl groups (Figure S1, Supporting Information). The carboxylate groups on the propionyl side chains were converted to *N*-methylamides, to represent the eventual amide linkage with the Lys Nϵ amine. The various rotamers of the heme propionate groups (14 total, 7 pairs of enantiomers) were energy-minimized, and the distances between the *N*-methylamide nitrogen and the His (95) Nϵ nitrogen were measured in each.

Two α-helical ($\phi = -58°$; $\psi = -47°$) 13-residue peptides were created: Ac-A_6HA_6-NHMe (to represent PSMs **1**−**4**) and Ac-A_2HA_{10}-NHMe (to represent PSM **5**). Each combination of ideal His χ_1 (180 and 300°) and χ_2 (90 and 270°) torsional angles[20] was set in both peptides, and the resulting structures were energy-minimized. Values of χ_1 and χ_2 before and after minimization in each model peptide are listed in Table 1, along with data from His residues which reside in helical regions of proteins.[21]

In the energy-minimized conformers of peptide Ac-A_6HA_6-NHMe, Lys was incorporated at positions $i \pm 4$ and $i \pm 3$ relative to His to represent the peptide components of PSMs **1**−**4.** In the conformers of peptide Ac-A_2HA_{10}-NHMe, Lys was incorporated at position $i + 7$ relative to His to represent PSM **5**. Lys torsional angles $\chi_1-\chi_4$ were set to all reasonable combinations[21] using ideal values of 60, 180, or 300°. The distance between His Nϵ2 and Lys Nϵ nitrogens was measured and compared to the distance between His (95) Nϵ2 and the amide nitrogen in each of the 14 heme propionate rotamers discussed above. In addition, the orientation of the Lys Nϵ nitrogen relative to the His Nϵ2 nitrogen was evaluated with the peptide oriented such that the His side chain was perpendicular to an imaginary plane (equivalent to the heme plane in the eventual PSM structures). The ideal arrangement has these two nitrogen atoms approximately equidistant above the plane. A given combination of His, Lys, and propionate torsional angles was assumed to be compatible with helicity if these distances differ by less than 1 Å. A more detailed description of the molecular modeling methods is available in the Supporting Information.

Table 1. Energy-Minimized His Side Chain Torsional Angles in Peptides Ac-A_6HA_6-NHMe and Ac-A_2HA_{10}-NHMe Compared with Average Values from Protein Helices[21]

torsional angle combination	starting His χ_1/χ_2 (deg)	min His χ_1/χ_2[a] (deg)	His in proteins χ_1/χ_2[b] (deg)
A	300/90	285.6/74.0	279(11)/95(26)
		312.6/129.4	
B	180/270	177.7/273.2	190(15)/239(19)
		183.4/279.0	
C	180/90	174.6/69.3	182(11)/82(37)
		178.6/69.5	
D	300/270	303.9/343.0	293(11)/273(56)
		302.7/277.0	

[a] Top line refers to Ac-A_6HA_6-NHMe. Bottom line refers to Ac-A_2HA_{10}-NHMe [b] For His residues in helical regions of proteins. Values in parentheses are standard deviations.

Circular Dichroism. CD experiments were performed on a JASCO 710 circular dichroism spectropolarimeter at 8 °C. The instrument is automatically calibrated with (1*S*)-(+)-10-camphorsulfonic acid. Temperature control was achieved using a circulating water bath. The actual temperature within the cell was measured using an Omega model HH200 thermometer with a K thermocouple (±0.2 °C accuracy). For all studies, cell path length (l) was 1.0 cm. Spectra in the far-UV (190−240 nm) represent the average of 3−5 scans, while those for the Soret band represent the average of 5−15 scans. Spectra in the far-UV are reported in terms of mean residue ellipticity ($[\theta]$, in deg·cm^2·dmol^{-1}), calculated as $[\theta] = [\theta]_{obs}(MRW/10lc)$ where $[\theta]_{obs}$ is the ellipticity measured in millidegrees, MRW is the mean residue molecular weight of the peptide (molecular weight divided by the number of amino acids), c = sample concentration in mg/mL, and l = optical path length of the cell in centimeters. Spectra in the Soret region are reported in terms of molar ellipticity ($[\theta]_{Soret}$, in deg·cm^2·dmol^{-1}), calculated as $[\theta]_{Soret} = [\theta]_{obs}(MW/10lc)$ where MW is the molecular weight of the compound. The fraction of helical peptide (f) was determined as described in ref 1.

Ultraviolet/Visible Spectroscopy. UV/vis spectra were recorded on a Kontron UVIKON 9410 recording spectrophotometer with a thermostated cell compartment. Temperature within the cell was measured using the Omega HH200 thermocouple. Quartz cuvettes with a path length of 1.0 cm were used for most measurements. Concentration studies of PSMs **1**−**5** were performed to investigate whether aggregation occurred. For these measurements, cuvettes ranging in length from 0.01 to 1 cm were employed. Spectra were run at a series of PSM concentrations between 10 μM and 2 mM (200-fold range) at 8 °C both in 2 mM phosphate buffer (pH 7) and in buffered aqueous solution containing 25% TFE (v/v). Plots of Soret ϵ_{max} vs PSM concentration were linear in all cases (not shown), demonstrating that the compounds exist as monomers over this concentration range.

Reduction of the iron(III) PSMs to iron(II) complexes in 50 mM phosphate buffer, pH 7.0, or mixtures of 50 mM phosphate buffer and TFE or PrOH (25% v/v) was accomplished as follows: A 25 mL portion of the appropriate solvent in a 50 mL round-bottomed flask was degassed by bubbling through a stream of nitrogen for 90 min. Solid sodium dithionite (1.5−2.0 mg) was added quickly, and nitrogen was bubbled through the resulting solution for an additional 15 min. An aliquot of the PSM sample (dissolved in water) was added to a 1.0 cm quartz cuvette, which was then fitted with a septum. The cuvette was purged with nitrogen until no water remained. The degassed dithionite solution (1.0 mL) was subsequently added to the dried PSM in the cuvette using a Hamilton gastight syringe.

pH Titrations. UV/vis titrations of PSMs **1**−**5** at a series of pH's were performed at sample concentrations ranging between 0.6 and 2.1 μM. The McIlvaine buffer system[22] (25 mM in H_2O or in 30% TFE (v/v) in H_2O) was used for data between pH 2.2 and 8. Buffers of pH

(18) Molecular modeling studies are performed using Sybyl moledular modeling software version 6.01, Tripos Associates, Inc., St. Louis, MO. Weiner, S. J.; Kollman, P. A.; Case, D. A.; Singh, U. C.; Ghio, C.; Alagona, G.; Profeta, S.; Weiner, P. *J. Am. Chem. Soc.* **1984**, *106*, 765−784.

(19) Bolognesi, M; Onesti, S.; Gatti, G.; Coda, A.; Ascenzi, P.; Brunori, M. *J. Mol. Biol*. **1989**, *205*, 529−544. The structure is registered as file pdb1mba in the Protein Data Bank, Brookhaven National Laboratory.

(20) Chakrabarti, P. *Protein Eng.* **1990**, *4*, 57−63.

(21) McGregor, M. J.; Islam, S. A.; Sternberg, M. J. E. *J. Mol. Biol.* **1987**, *198*, 295−310.

0.5, 1.0, and 1.5 were prepared by adjusting the pH of 25 mM citric acid with dilute hydrochloric acid. pH measurements were made with an Accumet model 10 pH meter equipped with a silver chloride electrode and are uncorrected for the 30% TFE samples. All samples were thermostated at 8.0 °C.

Electron Paramagnetic Resonance Spectroscopy. X-band EPR spectra were recorded on a Bruker ESP 300 with an Oxford Instruments ESR 900 liquid-helium cryostat. Spin concentrations of the samples were determined by comparing the doublly integrated intensities of the nonsaturated EPR signals against a Cu^{II}EDTA spin standard.

Fourier Transform Raman Spectroscopy. Steady state Fourier transform Raman spectra at 6 ± 2 °C were measured with a Bio-Rad Digilab FTS 60A interferometer. A Coherent Antares 76-YAG, with a repetition rate of 76 MHz (mode-locked), was used as a source of near-infrared (1064 nm) radiation. FT-Raman scattering was generated by 0.7 W, 1064 nm radiation and collected in backscattering geometry. Sample temperature at 6 ± 2 °C was maintained by flowing a water−ethylene glycol mixture through a home-built sample cell holder with a temperature controller (NESLAB, RTE-100). Sample temperature inside the sample was directly monitored with a probe before and after each spectral measurement. Symmetric interferograms at 4 cm^{-1} resolution were converted to corresponding spectra with a triangular apodization function. The FT Raman spectrum of the solvent was measured separately and subtracted from each sample spectrum with an appropriate subtraction factor to remove the solvent contribution.

Results and Discussion

Design of the PSMs. Design of the first generation of PSMs was based on three guiding principles: (1) the final structures should bear some resemblance to active sites of known hemoproteins; (2) the compounds should be water soluble; and (3) synthesis should involve a minimum of steps. The four new PSMs presented in this report (**2**−**5**) are isomers of **1**, which was the subject of a previous publication.[1] In **1** and **2**, Lys and His are separated by three amino acids (Lys−His separations of *i*, *i* + 4 and *i*, *i* − 4, respectively), the compounds differing only in that the peptide sequences are reversed. In PSM **1**, the Lys linker is located near the N-terminus of the peptide whereas, in **2**, it is positioned near the C-terminus. Compounds **3** and **4** are analogues of **1** and **2**, respectively, in which His has been moved one position closer to the Lys linker (Lys−His separations of *i*, *i* + 3 and *i*, *i* − 3, respectively). In PSM **5**, His is at position *i* − 7 relative to Lys. The peptides contain 13 amino acids, one more than the average length of protein helices,[23] and include 3 glutamic acid (Glu) residues for water solubility at neutral pH. The remaining amino acids, other than those involved in connections to the heme group, are helix-favoring alanines.[24] The N-termini are capped by acetyl groups, while the C-termini are primary amides. Because of the short length of the peptides employed, and the presence of the helix-breaking His, the peptides were expected[24] (and found) to adopt random coil conformations in aqueous solution. The monopeptide analogues of **2**−**5** (**2m**−**5m**) were prepared in order to better understand Fe−His coordination equilibria in the PSMs. We previously reported that **1** and **1m** exhibit essentially identical helix induction.[1]

Each PSM is expected to exist as a pair of diastereomers, due to the location of the propionate groups on pyrrole β positions that are related by a pseudo-C_2 rotation axis. Efforts are currently underway to generate analogues of **1**−**5** that exist as single stereoisomers (vide infra).[25] Nevertheless, the present systems serve as excellent starting points for probing the relationship between peptide structure and model hemoprotein properties.

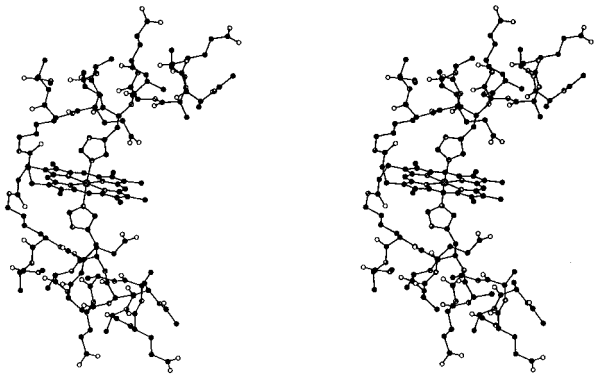

Figure 1. Structure of one diastereomer of PSM **2** predicted by molecular modeling studies. Atom shades are as follows: carbon (black); nitrogen (gray); oxygen (white).

Structural Predictions from Molecular Modeling Studies. Molecular modeling studies[18] led to several structural predictions for the limiting case where the peptides are fully helical. For PSM **1**, χ_1/χ_2 combination **A** (Table 1) gives good alignment between peptide and heme. With this combination, the peptide helix axis is nearly parallel to the heme plane, and the His Nδ1-H is free to hydrogen-bond with the backbone carbonyl of the amino acid at position *i* − 4.[20] Several Lys side chain conformations appear to be reasonably compatible with peptide helicity. For PSM **2**, combination **B** should be exclusively favored. In this arrangement, the Lys side chains make extensive van der Waals contact with the heme ring, as do the C-termini of the peptides. A structure predicted for one diastereomer of this compound is shown in Figure 1. A detailed description of the modeling of this molecule is provided in the Supporting Information.

For PSM **3**, only combination **C** provides a suitable orientation between His and Lys. However, the C-termini of the peptides make unfavorable steric interactions with the heme, and the Ala at position *i* + 1 relative to His meets a steric obstacle in the heme propionate group. Helix induction in **3** was thus predicted to be unlikely. For PSM **4**, combinations **A** and **B** both give good heme−peptide alignment, although combination **B** appears to be superior. Finally, for PSM **5**, only combination **A** need be considered. Because the resulting His−Lys separation is about 1.5 Å larger than the largest possible separation that can be accommodated by the heme, we expected little helix induction in **5**.

Factors Affecting Helix Induction in the PSMs. The extent of helix induction in each PSM will be a function of three major factors: (1) the ability of His, Lys, and propionate groups to adopt torsional angles that are compatible with a helical peptide; (2) whether the Fe−His bonds provide enough energy to overcome entropically disfavored restriction of torsional angles in the peptide backbone, His and Lys side chains, and heme propionate groups that accompanies helix induction;[26] and (3) competition between intrapeptide hydrogen bonds and hydrogen bonding of the peptide amides with water.[24] Other factors that may modulate the extent of helix content include interactions (favorable or unfavorable) between amino acid side chains and

(22) McIlvaine, T. C. *J. Biol. Chem.* **1921**, *49*, 183−186.
(23) Presta, L. G.; Rose, G. D. *Science* **1988**, *240*, 1632−1641.
(24) Scholtz, J. M.; Baldwin, R. L. *Annu. Rev. Biophys. Biomol. Struct.* **1992**, *21*, 95−118.
(25) An analogue of PSM **2** built from mesoporphyrin II was recently prepared: Wang, M.; Kennedy, M. L.; Hart, B. R.; Benson, D. R. *Chem. Commun.* **1997**, 883−884.
(26) (a) Schrauber, H.; Eisenhaber, F.; Argos, P. *J. Mol. Biol.* **1993**, *230*, 592−612. (b) Bobrik, M. A.; Walker, F. A. *Inorg. Chem.* **1980**, *19*, 3383−3390.

Table 2. Soret λ_{max} (nm) and Peptide Helix Content[a] as a Function of Solvent for PSMs **1**−**5**

PSM	λ_{max} (H_2O)	λ_{max} (25% TFE)	λ_{max} (25% PrOH)	$10^{-5}\epsilon_{max}$ (H_2O)
1	403.1 (49%)	401.3 (97%)	403.1 (97%)	1.28
2	402.9 (58%)	402.3 (95%)	403.7 (95%)	1.30
3	402.0 (≈5%)	401.1 (70%)	402.6 (50%)	1.32
4	402.6 (32%)	401.1 (80%)	402.7 (80%)	1.28
5	402.8 (18%)	401.5 (70%)	402.9 (80%)	1.31

[a] Peptide helix content of **1**−**5** is shown in parentheses after each λ_{max} value.

the heme face and β-substituents and the ability of the His imidazolyl group to adopt a favorable orientation relative to heme iron.[27]

Ultraviolet/Visible Spectroscopy of the Fe(III) Complexes of 1−5 and 1m−5m. UV/vis spectra of Fe(III)-PSMs **1**−**5** in 2 mM potassium phosphate buffer (pH 7), 25% TFE (v/v), and 25% PrOH (v/v) indicate that the iron atom is low spin, consistent with bis-His coordination[28] (spectra not shown; see ref 1 for a spectrum of **1**). Spectral features include the β (Q_v) and α (Q_o) bands near 525 nm and 565 nm and the Soret band in the vicinity of 400 nm (Table 2). Absence of large amounts of high-spin iron(III) is indicated by lack of a π-iron charge transfer band near 620 nm,[28] as well as by the weak or absent high-spin signal in EPR spectra of the compounds (vide infra). Factors responsible for the differences in Soret λ_{max} (Table 2) likely include hydrogen bonding to the His Nδ1 hydrogen (either intramolecular bonding or bonding with solvent molecules)[29] and orientation of the His imidazolyl groups relative to the heme (variation of the metal pπ−imidazole pπ overlap).[27c]

For the monopeptide systems **1m**−**5m**, typical high-spin spectra are observed featuring the charge transfer band at 620 nm, the high-spin β band (Q_v) at 495 nm, and the Soret band at 391 nm[28] (not shown; see ref 1 for a spectrum of **1m**). As previously reported for **1m**,[1] the spectra of all monopeptide systems exhibit concentration-dependent behavior, similar to what has been reported for the heme−peptide fragments of cytochrome *c*.[30] Thus, all measurements were made at or below 1 μM concentration. Spectra of **1**−**5** measured at pH 2 in water are also consistent with high-spin iron. Circular dichroism data discussed below indicate that the effect of acid is to prohibit the His side chains from acting as ligands toward the heme Fe(III). Thus, at low pH, H^+ can compete effectively with the intramolecular Fe for coordination to His. This is consistent with the known lability of Fe−His bonds in iron porphyrins to ligand-exchange, a process that occurs via a dissociative reaction.[31]

Electron Paramagnetic Resonance Spectra of the Fe(III) Complexes of 1−5. Frozen solution EPR spectra of the Fe(III) complexes of **1**−**5** (10 mM potassium phosphate buffer, pH 7.0, with 10% glycerol) recorded at 20 K are shown in Figure 2. The spectral shape and g values ($3.1 > g > 1.4$) indicate that **1**−**5** are low-spin Fe(III) complexes of low (rhombic) symmetry. The spin concentrations, determined by double integration, were nominally 0.7 mM for all samples, consistent with concentrations determined spectrophotometrically. The signal at $g = 5.8$ for samples **3** and **5** is from a high-spin minority Fe(III) species representing <5% of the total iron.

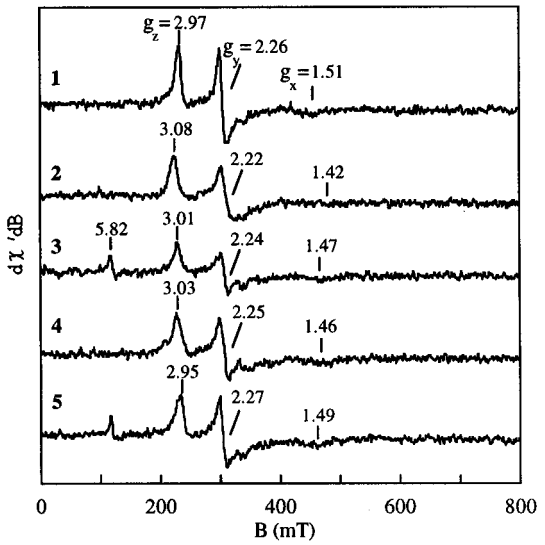

Figure 2. Frozen solution X-band EPR spectra of PSMs **1**−**5**, nominally 0.7 mM, in 10 mM phosphate buffer, pH 7.0. Instrumental parameters: temperature, 20 K; microwaves, 0.2 mW at 9.6 GHz; modulation, 10 G at 100 kHz.

Table 3. EPR Parameters of **1**−**5**

PSM	g_z[a]	g_y	g_x	Δ/λ[b]	V/Δ	ϕ[c]
1	2.97	2.26	1.51	3.33	0.55	29 ± 1
2	3.08	2.22	1.42	3.32	0.48	42 ± 5
3	3.01	2.24	1.47	3.32	0.52	34 ± 2
4	3.03	2.25	1.46	3.26	0.53	32 ± 3
5	2.95	2.27	1.49	3.19	0.58	23 ± 4

[a] All principal g values yielded a sum of the squares of the wave function coefficients that deviated from unity by less than 2%.[32b] [b] The errors in values of Δ/λ and V/Δ are ±0.15 and ±0.02, respectively, as determined from an estimation of the uncertainties in the positions of the resonances. [c] The errors in ϕ are due to the uncertainties in Δ/λ and V/Δ and to the uncertainty in the plot of ϕ vs V/Δ from Quinn et al.[34a]

The g values can be related to energy splittings of the spin-admixed t_{2g}-orbital states of a low-spin Fe(III) center via the Griffith model.[32] Values of Δ/λ and V/Δ for each complex were calculated using eq 8 of ref 32b, where Δ and V are the orbital energy splittings for tetragonal and rhombic distortions, respectively, and λ is the spin−orbit coupling constant (Table 3). An alternative set of $|\Delta/\lambda|$ and $|V/\Delta|$ values can be plotted on the low-spin heme correlation diagram of Blumberg and Peisach,[33] which relates the axial heme coordination to the orbital energy splittings. These alternate values of $|\Delta/\lambda|$ and $|V/\Delta|$ place **1**−**5** within the region of the correlation diagram for bis-His(ϵ) coordination.

A possible source for variation in the g values for **1**−**5** is differences in the angle ϕ between the plane of the His

(27) (a) Scheidt, W. R.; Lee, Y. J. *Struct. Bonding (Berlin)* **1987**, *64*, 1−70. (b) Collins, D. M.; Countryman, R.; Hoard, J. L. *J. Am. Chem. Soc.* **1972**, *94*, 2066−2072. (c) Nakamura, M.; Tajima, K.; Tada, K.; Ishizu, K.; Nakamura, N. *Inorg. Chim. Acta* **1994**, *224*, 113−124 and references therein.

(28) Adar, F. In *The Porphyrins*; Dolphin, D., Ed.; Academic: New York, 1978; Vol. 3, Chapter 2.

(29) (a) Traylor, T. G.; Popovitz-Biro, R. *J. Am. Chem. Soc.* **1988**, *110*, 239−243. (b) Chacko, V. P.; La Mar, G. N. *J. Am. Chem. Soc.* **1982**, *104*, 7002−7007. (c) Valentine, J. S.; Sheridan, R. P.; Allen, L. C.; Kahn, P. C. *Proc. Natl. Acad. Sci. U.S.A.* **1979**, *76*, 1009−1013. (d) Salemme, F. R.; Kraut, J.; Kamen, M. D. *J. Biol. Chem.* **1973**, *248*, 7701−7716. (e) Landrum, J. T.; Hatano, K.; Scheidt, W. R.; Reed, C. A. *J. Am. Chem. Soc.* **1980**, *102*, 6729−6735.

(30) (a) Carraway, A. D.; Povlock, S. L.; Houston, M. L.; Johnston, D. S.; Peterson, J. *J. Inorg. Biochem.* **1995**, *60*, 267−276. (b) Urry, D. W.; Pettigrew, J. W. *J. Am. Chem. Soc.* **1967**, *89*, 5276−5283.

(31) Satterlee, J. D.; La Mar, G. N.; Bold, T. J. *J. Am. Chem. Soc.* **1977**, *99*, 1088−1093.

(32) (a) Palmer, G. In *Iron Porphyrins*; Lever, A. B. P., Gray, H. B., Eds.; Addison Wesley: Reading, MA, 1980; Vol. 2, pp 43−88. (b) Taylor, C. P. S. *Biochim. Biophys. Acta* **1977**, *491*, 137−148.

(33) Blumberg, W. E.; Peisach, J. In *Probes of Structure and Function of Macromolecules and Membranes*; Chance, B., Yonetani,T., Mildvan, A. S., Eds.; Academic: New York, 1971; Vol. 2, pp 215−229.

imidazolyl side chains and the N−Fe−N bonds of the mesoheme (see Figure S4, Supporting Information). In work by Quinn et al.,[34] a series of structurally characterized bis(imidazole)-coordinated Fe(III) tetraphenylporphyrin complexes was examined with single-crystal and solution EPR spectroscopy. A correlation was observed between the rhombic distortion parameter V/Δ and the angle ϕ and attributed to a combination of metal to ligand π-interactions and pseudo-Jahn−Teller distortions.[34a] We have utilized this correlation to provide the estimates of ϕ for **1**−**5** given in Table 3. This correlation may not be generally applicable, given that frozen solution spectra can bias *g* values toward extremum in a distribution of configurations with different V/Δ values.[34] In an effort to minimize the effects of distributions, we have recorded EPR spectra both with and without glycerol. Glycerol tends to minimize distributions in protein samples by reducing stresss on the sample induced by ice structures. The spectra without glycerol tend to be broader and give *g* values that are approximately equal for all complexes. The spectra in glycerol are sharper and give reproducible shifts across the series **1**−**5**. Quinn et al. also noted an increase in the axial splitting parameter Δ with increasing ϕ and attributed this to the shortening of the axial metal−ligand bond as steric interactions with the porphyrin are minimized. While our values of Δ (Table 3) tend not to follow this trend, the large uncertainty in their measurement does allow for it.

Of all the PSMs, **2** experiences the largest helix induction. As a result, rotation about the His−Fe linkage may be more restricted in **2** than in the other PSMs. On the basis of the above discussion, more highly restricted rotation is a possible explanation for apparent adoption by **2** of a high-energy (larger) value of ϕ.[27a]

Circular Dichroism Analysis of Peptide Conformation. A fully helical peptide has the following characteristic CD features: a negative band corresponding to the amide n−π* transition in the vicinity of 220−222 nm and a negative band near 208 nm and a strong positive band near 190 nm resulting from exciton coupling of the amide $\pi-\pi$* transition.[35] The dominant feature in CD spectra of random coil peptides is a strong negative band below 200 nm.[35] The fraction of peptide helix (helix content; *f*) can be estimated from the mean residue ellipticity (MRE) in the region of 220−222 nm (θ_{obs}), as long as the MRE at the appropriate wavelength for the fully helical peptide (θ_{max}) and for the random coil peptide (θ_o) are known (see discussion in ref 1). It should be noted that the helix content measured in this manner does not take into account small contributions of the heme in the far-UV region, which we have previously demonstated to be present in CD spectra of **1**.[1] Estimated helix content for PSMs **1**−**5** in 2 mM potassium phosphate (pH 7) at 8 °C are listed in Table 2. Helix content of each PSM and its monopeptide analogue is identical within experimental uncertainty (±5%), indicating that in **1m**−**5m**, Fe−His coordination is energetically favorable at neutral pH. CD spectra of **1**−**5** in aqueous solution are shown in Figure 3. Spectra run in pH 2 buffer for all five PSMs are indicative of the peptides adopting random coil conformations, consistent with loss of both Fe−His bonds (spectra not shown; see ref 1 for a CD spectrum of **1** at pH 2). Loss of both ligands is also suggested by complete disappearance of the heme CD Soret signals for all PSMs at low pH (vide infra).

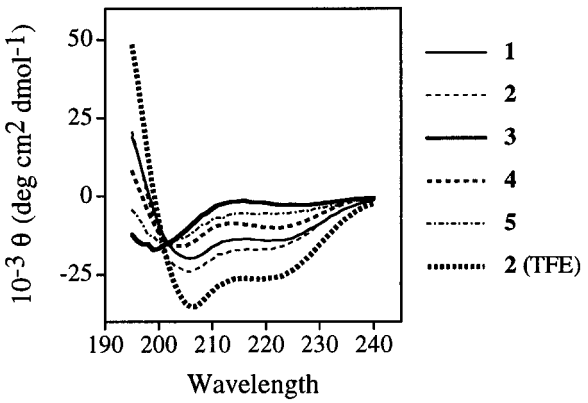

Figure 3. CD spectra of PSMs **1**−**5** in 2 mM phosphate buffer, pH 7, and of **2** in aqueous TFE (25% TFE, v/v) with 2 mM phosphate buffer (pH 7).

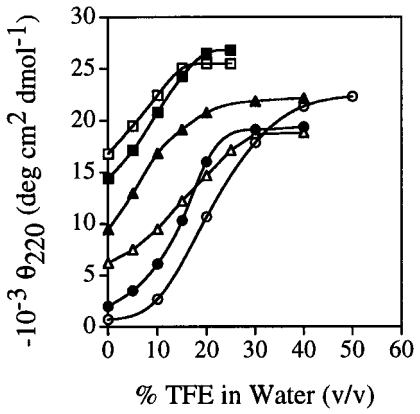

Figure 4. Circular dichroism data (8 °C) for **1**−**6** plotted as θ_{220} vs volume percent of TFE: **1** (closed squares); **2** (open squares); **3** (closed circles); **4** (closed triangles); **5** (open triangles); **6** (open circles). Sample concentrations ranged from 5 to 10 μM. Ellipticity for 100% helicity (θ_{max}) = 27 700 deg·cm^2·dmol^{-1}.

TFE is well-known for its ability to induce short peptides to adopt helical conformations.[36] In addition, TFE and other organic solvents are able to push helix−coil equilibria in the direction of the helix by favoring intramolecular hydrogen bonding. The CD spectrum of PSM **2** in aqueous TFE (25% TFE v/v) is shown in Figure 3. Data from TFE titrations of PSMs **1**−**5** and for model peptide **6**[1] are shown in Figure 4,

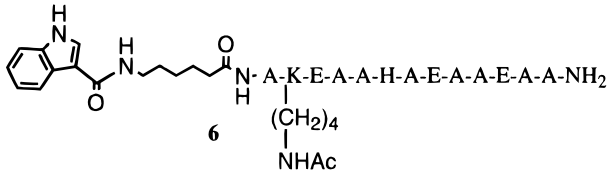

plotted as MRE at 220 nm (θ_{220}) vs volume percent of TFE. Titrations have also been performed with PrOH (not shown; data for **1** can be found in ref 1), which is nearly as effective as TFE at stabilizing peptide helices in the PSMs. The maximal estimated helix content for each PSM, reached in 25% TFE (v/v) or in 25−30% PrOH (v/v), is provided in Table 2. A plot of θ_{220} vs volume percent of TFE is markedly sigmoidal for **3**, indicating that the peptides in this compound are not in a helix-coil equilibrium in aqueous buffer (Figure 4).[37] This behavior is similar to that exhibited by **6**[1] (Figure 4). PSM **5**

(34) (a) Quinn, R.; Valentine, J. S.; Byrn, M. P.; Strouse, C. E. *J. Am. Chem. Soc.* **1987**, *109*, 3301−3308. (b) Walker, F. A.; Huynh, B. H.; Scheidt, W. R.; Osvath, S. R. *J. Am. Chem. Soc.* **1986**, *108*, 5288−5297.
(35) Woody, R. W. In *The Peptides*: *Analysis, Synthesis, Biology*; Hruby, V. J., Ed.; Academic: Orlando, FL, 1985; Vol. 7, Chapter 2.
(36) (a) Cammers-Goodwin, A.; Allen, T. J.; Oslick, S. L.; McClure, K. F.; Lee, J. H.; Kemp, D. S. *J. Am. Chem. Soc.* **1996**, *118*, 3082−3090. (b) Lesk, A. M.; Chothia, C. *J. Mol. Biol.* **1980**, *136*, 225−270.
(37) Jasanoff, A.; Fersht, A. R. *Biochemistry* **1994**, *33*, 2129−2135.

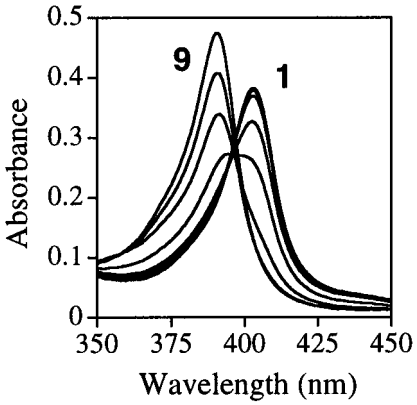

Figure 5. UV/vis spectra of PSM **1** as a function of pH. Spectrum 1: pH 7.4. Spectrum 9: pH 2.4

also exhibits sigmoidal behavior, although it is less prominent than for **3** or for **6**.

The high helix content for **1** and **2** (and for **1m** and **2m**) in neutral aqueous solution is consistent with predictions from molecular modeling studies, whereas helicity in **4** and **4m** was somewhat lower than expected. The low helix content in **5** and **5m**, and the absence of helix in **3** and **3m**, presumably results because the His and Lys side chains in these compounds are less able to adopt orientations that are compatible with a helical peptide, as predicted in molecular modeling studies.

Heme Features in CD Spectra. As was reported for **1**,[1] all five Fe(III)-PSMs exhibit induced CD spectra in the heme Soret region,[38,39] which are extremely sensitive to peptide conformation (not shown; see ref 1 for a spectrum of **1**). The monopeptide adducts **1m**−**5m** also exhibit heme CD Soret bands, shifted to ca. 391 nm as expected on the basis of UV/vis spectra.

When the PSMs are examined in aqueous solution at pH 2, conditions under which UV/vis spectra indicate that the Fe(III) is high-spin (vide infra), the Soret CD bands disappear. Coupled with complete loss of peptide helicity in **1**, **2**, **4**, and **5** under the same conditions, these data support the interpretation that at pH 2 neither His remains coordinated to Fe.

pH Titrations of Fe(III)-PSMs of 1−**5.** The effect of acid on Fe(III)-PSMs **1**−**5** was examined in aqueous solution and in 30% TFE at 8 °C by UV/vis spectroscopy. Decrease in intensity of the Soret band (ca. 403 nm) of low-spin heme was followed as a function of pH (Figures 5 and 6).

The various Fe−His coordination equilibria and His protonation equilibria involved in the pH titrations are shown in eq 1. In eq 1, His that is not coordinated to Fe is indicated by a

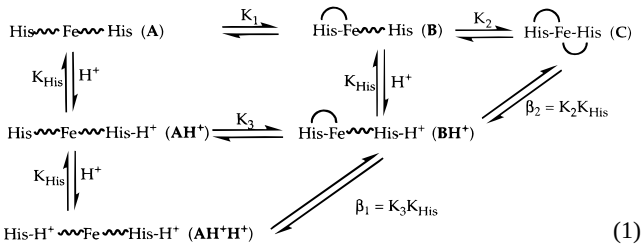

(1)

jagged line. Coordination of His to Fe is indicated by a curved line above His and Fe. When Fe(III) porphyrins are titrated with imidazole, no monoimidazole-coordinated Fe(III) porphyrin (compare **B** in eq 1) is observed. This results because $K_2 >> K_1$, allowing the product of the association constants (K_1K_2) to be determined using a two-state equilibrium model.[40]

We noted above that there is no difference in peptide helix content between each PSM and its monopeptide analogue at pH 7 in water. This indicates that, for the PSMs, in neutral solution, **B** (eq 1) is more stable than **A** ($K_1 >> 1$). From EPR spectra we have seen that bis-His coordination is strongly favored in neutral aqueous solution for all five PSMs. Thus, under these conditions, **C** is more stable than **B** ($K_2 >> 1$). The value of β_2 (K_2K_{His}; eq 1) at pH 7.0 is ≥20 for **3** and **5**, on the basis of the observation of ≤5% high-spin Fe in their EPR spectra. The value will be even larger for **1**, **2**, and **4**, for which no high-spin signals are seen. Because the His pK_a is ca. 7, at neutral pH, noncoordinated His would be about 50% protonated. His protonation under neutral conditions thus cannot compete effectively with intramolecular coordination of His to Fe. This is due to the high local concentration of Fe relative to His, a classic chelate effect. However, as the pH is lowered below the pK_a of His, competition becomes favorable. This is indicated by a change from low-spin to high-spin Fe(III) porphyrin in the UV/vis spectra of **1**−**5** with decreasing pH and by decreasing ellipticity at 403 nm in the CD spectra of **1**, **2**, and **4** with decreasing pH. At the acidic end of the pH titrations, neither His ligand is coordinated to Fe, as evidenced by CD (vide supra).

We observe small deviations from isosbesticity in each UV/vis titration. One factor that may contribute to this behavior is that each PSM exists in two diastereomeric forms (the values of β_1 and β_2 for one diastereomer are expected to be similar, though not identical, to the values for the other diastereomer). In addition, it is possible that some self-association occurs at lower pH as the hydrophobic porphyrin becomes exposed to the bulk solvent (as suggested by the strong concentration dependence exhibited by the monopeptide systems). As a result, we are unable to determine β_1 and β_2 (and thus K_1 and K_2) accurately. However, examination of the data in Figure 6 shows that acid sensitivity of the PSMs is quite variable. A shift in the midpoint of a pH titration to a lower pH is expected to correlate with higher values of both K_1 and K_2 (eq 1).

Sensitivity to acid in aqueous solution at 8 °C, as indicated by the midpoint of the pH titrations, falls in the order **5** > **3** > **2** > **1** > **4**. The higher sensitivity of **3** and **5** to H^+ in aqueous solution than of **1**, **2**, and **4** is consistent with the observation of a high-spin signal in their EPR spectra at neutral pH. In 30% TFE, the order is **5** > **3** > **1** ≈ **2** ≈ **4**. In 30% TFE, there is a large disparity between the behavior of **3** and **5** in comparison to the other three PSMs.

The position of the Fe−His coordination equilibrium in each PSM will be determined by a variety of thermodynamic factors. The combination of factors that leads to the overall lowest energy in a particular PSM (under a given set of conditions) will prevail. For example, adoption of an unfavorable orientation of His relative to the heme (ϕ) may occur without a marked change in stability toward acid if other factors are present that can stabilize the folded form of the PSM relative to the unfolded form (such as hydrophobic interactions between amino acid side chains and the heme). In other words, the overall stability of a folded PSM is dependent not solely on the intrinsic Fe−His bond strength but rather on the sum total of interactions that accompany formation of the folded PSM. This concept is most impressively demonstrated in hemoproteins such as hemoglobin, in which binding of heme is almost completely governed by hydrophobic interactions. In a relevant recent example, helix

(38) Blauer, G.; Sreerama, N.; Woody, R. W. *Biochemistry* **1993**, *32*, 6674−6679 and references therein.
(39) Mizutani, T.; Ema, T.; Yoshida, T.; Renne, T.; Ogoshi, H. *Inorg. Chem.* **1994**, *33*, 3558−3566.
(40) (a) Satterlee, J. D.; LaMar, G. N.; Frye, J. S. *J. Am. Chem. Soc.* **1976**, *98*, 7275−7282. (b) Hasinoff, B. B.; Dunford, H. B.; Horne, D. G. *Can. J. Chem.* **1969**, *47*, 3225−3232.

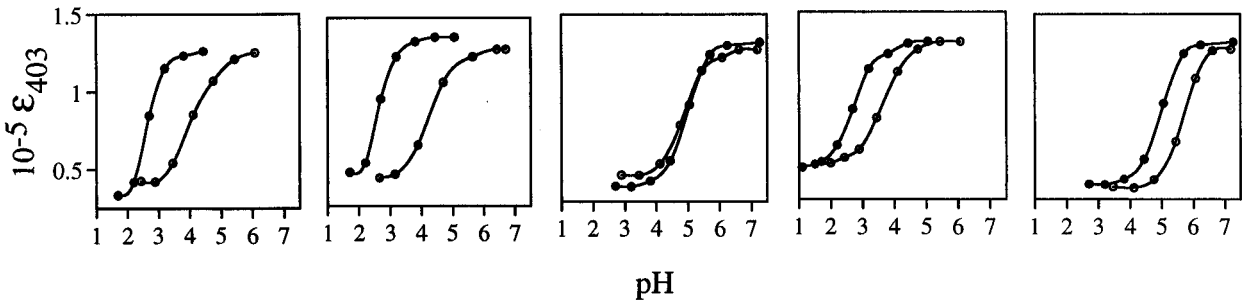

Figure 6. Plots of extinction coefficient (ϵ) at Soret λ_{max} vs pH for PSMs **1**−**5** in aqueous solution (open circles) and in 30% (v/v) TFE (closed circles). All spectra were recorded at 8 °C.

induction in a metal-free peptide−porphyrin adduct similar to PSM **4** occurs solely as the result of favorable hydrophobic interactions between the peptide and the porphyrin.[4b]

For **1**, **2**, **4**, and **5**, acid sensitivity appears to have a modest dependence on the number of amino acid residues separating His from the covalently attached Lys. This suggests that the extent of Fe−His coordination equilibrium is partly determined by the magnitude of the chelate effect (local effective ligand concentration) in each compound. The lower stability of **2** toward H^+ relative to **1** may result partially from an unfavorable value of ϕ (as measured by EPR; Table 3), which is suggestive of higher energy Fe−His bonds. The midpoint in the titration of **3** is about 1 pH unit higher than for **4**, even though in both compounds His is three residues removed from the Lys anchor. The EPR spectra of **3** and **4** are nearly identical, indicating similar values of ϕ (Table 3) and thus suggesting similar intrinsic Fe−His bond strengths. However, helicity is induced upon Fe−His bond formation in **4**, whereas in **3** the peptides remain in random coil conformations with reduced conformational freedom. Fe−His bond formation is in both cases entropically unfavorable. On the basis of the discussion in the previous paragraph, we suggest that for **4** this entropy loss is favorably offset by stabilizing interactions in **4** that are not available to **3**. These may include intrahelical hydrogen bonding. Once again, other factors may be important as well, for example differences in solvation of **3** and **4** or differences in intramolecular hydrophobic interactions.

The folded forms of the PSMs should be greatly stabilized in aqueous TFE, because peptide helicity will be favored whether or not the Fe−His bonds are intact (e.g., peptide **6** has ca. 80% helix content in 30% TFE[1]). As a result, changes in peptide conformation upon Fe−His bond formation in aqueous TFE will be much less dramatic. This is certainly the case for PSMs **1**, **2**, and **4**, which are markedly more stable to acid in 30% TFE than under purely aqueous conditions (Figure 6). These three PSMs exhibit nearly identical stability toward acid in 30% TFE. However, PSMs **3** and **5** are significantly less stable toward acid in 30% TFE than are **1**, **2**, and **4** (Figure 6). This again can best be described in terms of a chelate effect: when the peptides in the PSMs are helical, the local concentration of His relative to Fe is much higher than when the peptides have random structures. For **1**, **2**, and **4**, His and Lys are able to adopt side chain conformations that allow ready formation of an Fe−His bond when the peptides are helical, as predicted in molecular modeling studies. The higher local ligand concentration is not as advantageous for **3** and **5** in 30% TFE, because for His to coordinate to iron in these compounds the His or Lys side chains, and/or some segment of the peptide backbone, must adopt energetically unfavorable conformations. In **3** and **5**, additional interactions are not sufficient to effectively counteract the resulting Fe−His bond strain.

The springboard strain concept introduced by Traylor[12a] is an excellent analogy to use in discussing the PSMs. In aqueous solution, springing open results when the peptides unfold from partially helical conformations to random coils (or in the case of **3**, from a constrained to a less constrained random coil). The energetic advantage of springing open in **1**, **2**, and **4** is reduced when organic cosolvents are present. Increasing the peptide helix content in **3** and **5** with TFE or PrOH does not lead to large stabilization of the folded forms of these PSMs.

Table 4. Soret λ_{max} (nm) of Iron(II) PSMs **1**−**5**

PSM	λ_{max} (H_2O)	λ_{max} (25% TFE)	λ_{max} (25% PrOH)
1	411.0	409.4[a,b]	411.2[a,b]
2	410.9	410.2	411.9
3	410.1[a]	410.6[a]	411.9[a]
4	410.5	409.4	411.1
5	411.0[a]	410.2[a]	411.4[a]

[a] A shoulder is observed near 420 nm. [b] The Soret shoulder for this sample is minor.

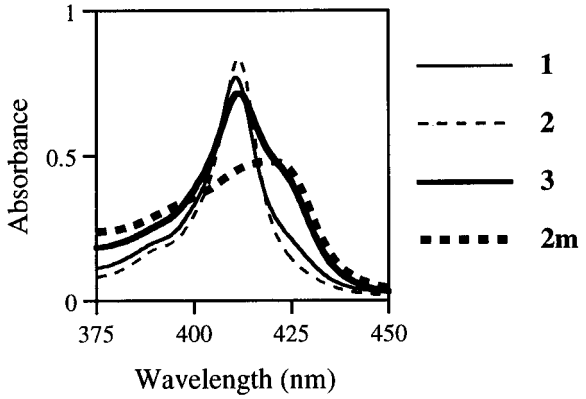

Figure 7. Soret region UV/vis spectra at 8 °C of iron(II) complexes of **1**, **2**, and **2m** in 50 mM phosphate buffer (pH 7)/PrOH (3:1) and of **3** in 50 mM phosphate buffer (pH 7). Sample concentrations are 5−6 μM.

Fe(III) to Fe(II) Reduction. In many hemoproteins, e.g. hemoglobin, myoglobin, and guanylate cyclase, iron exists in the ferrous oxidation state. We thus experimented with reduction of the Fe(III)-PSMs to Fe(II) complexes, accomplished using sodium dithionite in the absence of air. The Soret λ_{max} shifts to longer wavelengths by ca. 9 nm in each case (compare Tables 2 and 4), and low-spin α (ca. 547 nm) and β (ca. 518 nm) bands appear in the visible region.[28] The spectrum of PSM **2** is shown in Figures 7 (Soret region) and 8 (visible region). A sizeable shoulder is observed near 420 nm in aqueous buffer, 25% TFE, and 25% PrOH for PSMs **3** (Figure 7) and **5** (data not shown).

A smaller shoulder is observed for PSM **1** in 25% TFE and in 25% PrOH (Figure 7), its intensity increasing with temperature (not shown). There is no shoulder at 420 nm for PSMs **2** and **4** at 8 °C, although one grows in at higher temperatures. When **2m** is reduced in 25% PrOH, the Soret band shifts from

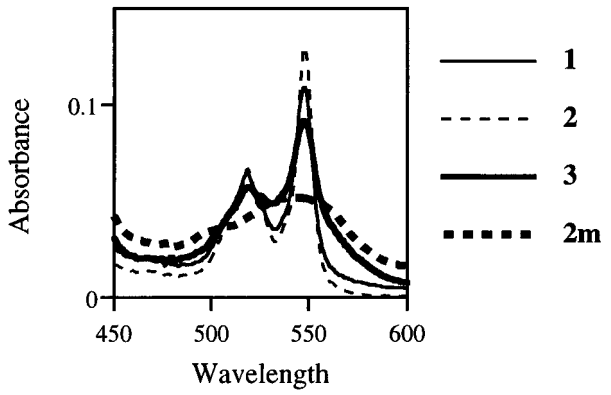

Figure 8. Visible spectra at 8 °C of iron(II) complexes of **1**, **2**, and **2m** in 50 mM phosphate buffer (pH 7)/PrOH (3:1) and of **3** in 50 mM phosphate buffer (pH 7). Sample concentrations are 5−6 μM.

390 to 419 nm (Figure 7). Traylor has reported five- and six-coordinate chelated mesohemes (fifth and sixth ligands are *N*-alkylimidazoles) with Soret bands at 417 and 407 nm, respectively.[41] In addition, the Soret band of myoglobin reconstituted with Fe(II) mesoporphyrin IX (which by comparison to X-ray structures of the native proteins should have a five-coordinate heme) occurs at 422.5 nm.[42] Thus, the Soret shoulders suggest that Fe(II)-PSMs **3** and **5** exist as an equilibrium mixture of five- (high-spin) and six-coordinate (low-spin) iron(II). Further evidence of five-coordinate heme in PSMs **3** and **5** is seen in the visible region of the spectrum. In PSM **2** (Figure 8) and **4** (not shown), the α and β bands are separated by a deep valley, and the long-wavelength edge of the α band departs sharply from the baseline. Spectra with similar features have been reported for other bis-His-coordinated complexes of Fe(II) porphyrins. In contrast, the visible bands of **3** (Figure 8) and **5** (not shown) appear to sit atop a separate broad absorbance centered between the α and β peaks. A corresponding broad absorbance in this region is observed in the spectrum of **2m** (Figure 8).

As demonstrated in Traylor's strained bis-chelated mesohemes,[43] and in complexes of hindered bases such as 2-methylimidazole,[40a,44] coordination of a second ligand to iron(II) porphyrins is weaker than coordination of the first, contrary to the situation with unstrained iron(II) porphyrins and with most iron(III) porphyrins. The observation of five-coordinate heme for the Fe(II) complexes of **3** and **5** strongly suggests that the folded forms of these PSMs are much less stable than the folded forms of **1**, **2**, and **4**. This is consistent with our findings for the Fe(III) complexes described above.

Raman Spectroscopy of PSMs 2 and 3. The steady state FT Raman spectrum of the Fe(III) complex of PSM **2** (5 mM) in 10 mM phosphate buffer at 6 ± 2 °C is displayed in Figure 9. Several core-size marker bands for PSM **3** in buffer and in 25% TFE are listed in Table 5. The spectra bear strong resemblance to previously recorded Raman spectra of the bis-(imidazole) complex of iron(III) mesoporphyrin IX,[45] also shown in Table 5. They are also similar to Raman spectra of cytochromes.[46] In particular, the oxidation state marker band

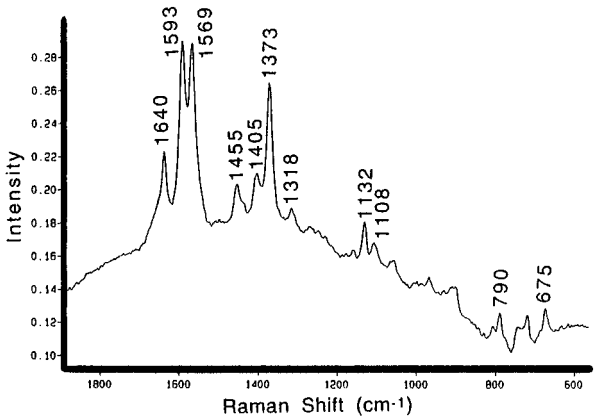

Figure 9. FT Raman spectrum of Fe(III)-PSM **2** (5 mM) in 10 mM phosphate buffer (pH 7), $T = 6 \pm 2$ °C. The excitation power was 0.7 W; total scan time 7 h; resolution 4 cm^{-1}. The FT Raman spectrum of the buffer was subtracted from the sample spectrum.

Table 5. Core Marker Bands (cm^{-1}) of PSM **3** Compared with the Bis(imidazole) Complex of Iron(III) Mesoporphyrin IX (FeMPIX)

Raman band	FeMPIX	PSM **3** (H_2O)	PSM **3** (TFE)
ν_{10}	1640	1641	1641
ν_2	1599	1594	1595
ν_{11}	1572	1570	1571
ν_4	1375	1374	1375

(ν_4) and several core-size marker bands (ν_{10}, ν_{11}, and ν_2) are present. An additional band at 1652 cm^{-1} is present in the spectra run in TFE solution, which we tentatively identify as the peptide amide I vibration. Spectra of these PSMs in aqueous buffer and in the presence of 25% TFE (v/v) are nearly identical.

The high-frequency region (1000−1700 cm^{-1}) of FT Raman spectra of PSMs is dominated by stretching vibrations. These vibrations are assigned to $C_\beta-C_\beta$, $C_\alpha-C_m$, and $C_\alpha-N$ bonds, C_β substituent, and $C_\alpha-C_\beta$ bonds and to C_m-H in-plane bending[47] (C_α and C_β are the inner and outer carbon atoms of the pyrrole ring, C_m is the methine bridge carbon, N is the pyrrole nitrogen, and H the methine bridge hydrogen). These core marker bands are extremely sensitive to changes in heme geometry, including nonplanar porphyrin distortions.[48] In the CD spectra of **3**, the heme Soret signal became split (one positive peak and one negative peak) as peptide helicity was induced by TFE (not shown). This suggested to us the possibility that helix induction in **3** was accompanied by a nonplanar distortion of the porphyrin. However, the minimal differences observed for spectra of PSMs **2** and **3** in aqueous buffer and in buffered aqueous/TFE solution speak strongly against this possibility. This is in keeping with the high energy required to distort iron porphyrins.[49]

Future Directions. Complete understanding of the influence of peptide conformation on heme properties, and vice versa, demands ultimately that compounds existing as single stereoisomers be developed. In order to achieve this goal, mesoporphyrin II (**7**) was recently synthesized[50] and the corresponding analogue of PSM **2** has been prepared.[25] We are also in pursuit of monophenyl- or tetraphenylporphyrin scaffolds for PSM construction. Because the phenyl rings would occupy

(41) Traylor, T. G.; Chang, C. K.; Geibel, J.; Berzinis, A.; Mincey, T.; Cannon, J. *J. Am. Chem. Soc.* **1979**, *101*, 6716−6731.
(42) Harbury, H. A.; Cronin, J. R.; Fanger, M. W.; Hettinger, T. P.; Murphy, A. J.; Myer, Y. P.; Viniogradov, Y. *Proc. Natl. Acad. Sci. U.S.A.* **1965**, *54*, 1658−1664.
(43) Geibel, J.; Chang, C. K.; Traylor, T. G. *J. Am. Chem. Soc.* **1975**, *97*, 5924−5926.
(44) Collman, J. P.; Reed, C. A. *J. Am. Chem. Soc.* **1973**, *95*, 2048−2049.
(45) Spiro, T. G.; Burke, J. M. *J. Am. Chem. Soc.* **1976**, *98*, 5482−5489.
(46) Cartlin, B. In *Biological Applications of Raman Spectroscopy* ; Spiro, T. G., Ed.; Wiley: New York, 1988; Vol. III, pp 217−248.
(47) (a) Kitagawa, T.; Abe, M.; Ogoshi, H. *J. Chem. Phys.* **1978**, *69*, 4516. (b) Abe, M.; Kitagawa, T.; Kyogoku, Y. *J. Chem. Phys.* **1978**, *69*, 4526.
(48) Shelnutt, J. A.; Majumder, S. A.; Sparks, L. D.; Hobbs, J. D.; Medforth, C. J.; Senge, M. O.; Smith, K. M.; Miura, M.; Luo, L.; Quirke, J. M. E. *J. Raman Spectrosc.* **1992**, *23*, 523−529.
(49) Hobbs, J. D.; Shelnutt, J. A. *J. Protein Chem.* **1995**, *14*, 19−25.
(50) Paine, J. B., III; Hiom, J.; Dolphin, D. *J. Org. Chem.* **1988**, *53*, 2796−2802.

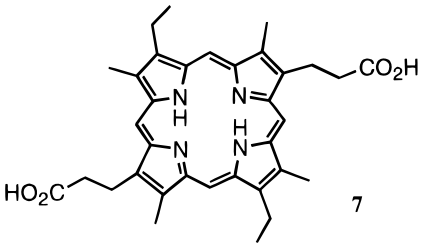

7

meso positions, two peptides attached to a single phenyl group would lead to a single stereoisomer with C_2 symmetry. Progress in this area will be reported in due course.

Conclusion

Stability of the folded forms of the PSMs is controlled by several factors. At the simplest level, it is related to the distance separating the His ligand from the covalently attached Lys, an example of the classic chelate effect. Modulating the chelate effect are the change in peptide conformation and the introduction of interactions between the peptide and the porphyrin that accompany Fe−His bond formation. This is dramatically illustrated by the effect of TFE on the acid sensitivity of **1**, **2**, and **4**: for these PSMs, helix stabilization provided by TFE or PrOH greatly increases the local concentration of His relative to Fe. In other words, the organic solvent prevents the helix from unfolding (springing open) when the Fe−His bonds break, as occurs in aqueous solution. In this respect, the cosolvent acts as a surrogate for the structural constraints normally imposed by the 3-D fold (or rack)[6] of apohemoproteins. For hemoproteins the rack also serves to define the geometry of coordinating His ligands, in some cases leading to strained Fe−His bonds that are vital to hemoprotein function. As demonstrated in this report, in the presence of organic cosolvent the Fe−His bonds of **3** and **5** still have a strong tendency to spring open, even though the helix content of the peptides has been substantially increased relative to aqueous solution. The strained Fe−His bonds result because the His and Lys residues cannot adopt low-energy conformations that are compatible with a helical peptide. A major difference between PSMs and hemoproteins is that the protein rack of the natural systems prohibits ligand dissociation. For **3** and **5**, then, strain simply results in increased Fe−His ligand exchange relative to the case of the other PSMs. Work is underway to create a series of PSM analogues in which the peptides have been linked together so as to eliminate the possibility of complete peptide unfolding. It will be of interest to examine how Fe−His bond strain is manifested in such conformationally locked hemoprotein models.

Acknowledgment. This work was supported by National Institutes of Health Grant R29-GM52431-01A1 and National Science Foundation EPSCoR Grant OSR-9255223 (the U.S. Government has certain rights in this material). The NSF-funded work received matching support from the State of Kansas. D.J.B. acknowledges summer support from the NSF Research Experiences for Undergraduates (REU) Program. We thank Professors Carey K. Johnson and F. Ann Walker for helpful discussions.

Supporting Information Available: A detailed textual description of molecular modeling methods used in structure predictions for PSMs **1**−**5**, with four figures (4 pages). Ordering information is given on any current masthead page.

IC960444P